

# Stability Analysis of Large Section Rocky Tunnel Support Structure

Chaofan Si, Jinhai Gao, Yahui Li

College of Energy Science and Engineering, Henan Polytechnic University, Jiaozuo, China

Email: sichaofan666@163.com

**How to cite this paper:** Si, C.F., Gao, J.H. and Li, Y.H. (2023) Stability Analysis of Large Section Rocky Tunnel Support Structure. *World Journal of Engineering and Technology*, 11, 234-245.  
<https://doi.org/10.4236/wjet.2023.112016>

**Received:** February 28, 2023

**Accepted:** April 25, 2023

**Published:** April 28, 2023

Copyright © 2023 by author(s) and Scientific Research Publishing Inc. This work is licensed under the Creative Commons Attribution International License (CC BY 4.0).

<http://creativecommons.org/licenses/by/4.0/>



Open Access

## Abstract

In order to study the stress characteristics of the initial support and secondary lining of the large section tunnel and to solve the problem of secondary lining cracking during operation. Taking the large section tunnel in Zihong village, Qi County as the research object, a numerical simulation method was used to establish a finite element model of the large section tunnel. So as to simulate and analyze the stress characteristics of the support structure of this tunnel. Through the simulation of the initial support and second lining of this large section tunnel in terms of displacement, stress, plastic zone damage and anchor shaft force, the results show that as the excavation progresses, the stress and displacement on the surface of the newly excavated tunnel profile is faster, especially at the side walls and arch footings, the stress and displacement values are slightly larger than other characteristic points, but the final values are stable and converge, and are basically consistent with the field monitoring results, which indicates that this support system is basically in stable state. Therefore, during the tunnel excavation and support process, special attention should be paid to the stability of the sidewalls and footings, and the results of this study will be of great practical significance for tunnel construction and maintenance.

## Keywords

Large Section Tunnel, Initial Support, Secondary Lining, Numerical Simulation, Stability

## 1. Introduction

With the rapid development of road traffic construction in recent years, tunnels play a vital role in the construction of mountainous highway tunnels or railroad tunnels. China's territory is vast, and the mountainous area accounts for two-thirds of the country's land area. Therefore, in the complex geological environ-

ment of mountainous areas, in order to reduce detours, it is necessary to build tunnels, of which road tunnel projects occupy a large part. During the operation of mountain highway tunnels, various problems may be encountered, among which concrete cracking of the secondary lining is a safety issue worthy of in-depth study.

The mechanical behavior of initial support and secondary lining of tunnels has been studied by scholars at home and abroad. Amorim [1] studied the cracking of secondary lining of tunnels based on damage mechanics from the perspective of concentrated load and uniform load, respectively. Jia Jianqing [2] took the section at 10 m from the cave entrance of Fangdoushan tunnel as an example, and analyzed the variation law of stress, displacement and anchor shaft force between primary support and secondary lining at this section by using numerical simulation and field monitoring. Di Chen [3] analyzed the lining cracking in the grade II section of the Lin Pan Shan tunnel by using numerical simulation and field monitoring, and proposed engineering countermeasures for preventing lining cracking. Huang Hongwei [4] studied the crack distribution law and occurrence mechanism by using the extended finite element method based on the field investigation and a large number of case studies. ZHANG Z [5] studied the effect of the change of construction method during tunnel construction on the initial lining after excavation based on the shallow buried large section tunnel in Jiaoweiqin. ZHAG X [6] used the discrete element simulation technique to establish a computational model to simulate and analyze the force characteristics of the secondary lining at different time periods. Qian FANG [7] investigated the pressure of initial support and second lining contact at different surrounding rock levels by using the method of field monitoring, and analyzed the force characteristics of the second lining, which provided great reference value for more scientific design of the second lining. Shao Zhushan [8], based on the Jinbunwan Tunnel of Jihu Expressway, analyzed the structural mechanical properties of tunnel surrounding rock stress and primary support by using ANSYS, which provided a more comprehensive basis in the optimal support timing of secondary lining. Based on Baoding 2 tunnel, Kang, Haibo [9] used numerical simulation and field tests to conclude that the coal seam intersecting the tunnel axis could more obviously affect the displacement of the tunnel vault and arch waist. Zhao Qichao [10] selected Qingyunshan tunnel for a 1:30 similar simulation experiment and explored the variation law of the lining structure inside a large section tunnel in a water-rich area. Chao Wu [11] used active loading to simulate the characteristics of the force, deformation and damage law of the secondary lining during the tunnel operation period. However, the cracking of secondary lining is affected by a variety of factors, and each inducing factor occupies a different proportion in different geological environments, so targeted research is needed for specific geological situations. Using field tests and numerical simulations, Dongqiang Xu [12] proposed the alternative method of adding foundation beams at the bottom of the elevated arch that can also meet the stability requirements.

In the case of complex geological conditions and chaotic fissure development in the tunnel site area, reasonable construction methods and second lining support will effectively solve the problem of second lining cracks during tunnel operation. Therefore, based on this paper, and based on the No. 1 tunnel in Zihong, Shanxi, an in-depth study of initial support and second lining will be conducted, and the findings will be of practical and positive significance for the study of tunnel excavation and rock support problems.

## **2. Project Overview**

Zihong No. 1 tunnel is in the fifth contract section of the new construction project of the first-class highway from Changjiazhuang, Qingxu County to Changzhi Border, Jinzhong City, Shanxi Province. The total length of the left line is 1221 meters, and the total length of the right line is 1237 meters. The tunnel is separated two-way 4 lanes, the design speed is 60 km/h. The starting point of this contract section is located in the east side of Zuojiatan village, and the end point is located in the end of Zihong No. 1 tunnel, the total length of the route is 1.875 km, and the maximum burial depth is 156.82 m.

### **2.1. Physical Geography Overview**

The tunnel site area has been influenced by natural factors for a long time, due to long-term tectonic denudation, the top of the mountain is rounded, mostly into a bun shape, the beam is relatively gentle, but narrower, the ridge is continuous, the slope is mainly steep, the mountain body is generally northwest to southeast direction. The direction of the proposed tunnel is basically the same as that of the mountain beam. The tunnel site area is well covered with vegetation, and the highest elevation is 1121.00 m. The relative height difference of the tunnel site area is 134.34 m, located in temperate continental monsoon climate, semi-arid state area.

### **2.2. Hydrogeological Conditions**

Due to the influence of rock yield and soil pore space, the groundwater runoff in the tunnel site area is mainly vertical runoff, and may be transformed into horizontal runoff only when encountering the relative water barrier. Eventually, owing to the hydrogeological conditions, it exists mainly in the form of interstratified water.

### **2.3. Engineering Geological Layer Characteristics**

The tunnel envelope is mainly composed of T1h sandstone, T2e sandstone and mudstone, with only a small amount of Quaternary Holocene artificially deposited (Q4ml) miscellaneous fill at the exit, and the overall rocky tunnel. The tunnel site area is relatively gentle, the seismic activity is relatively weak, the degree of damage is relatively light, there is no ground subsidence, ground cracks and other geological hazards in the tunnel site area, the impact on the proposed tunnel is relatively small. The physical and mechanical parameters of the tunnel

surrounding rock are shown in **Table 1**.

### 3. Numerical Simulation of the Stability of the Support Structure

#### 3.1. Modeling

In this study, Rhino was used to build the model, and the Flac3D finite difference program was used for numerical simulation and post-calculation of the figure. The primary support of the tunnel mainly used C25 concrete, anchor rods and steel arch structure support form. The support of the second lining used C30 concrete with the parameters shown in **Table 2**, and the mechanical parameters of the anchor rods shown in **Table 3**.

According to the actual project profile, the section at a distance of 50 m from the cave entrance is taken as an example. According to St. Venant's principle, the area around the center point of the section after excavation 3 to 5 times will be affected by the redistribution of stress in the surrounding rock [13]. Therefore, the model uses hexahedral solid units. The left and right are taken as 70 m. The tunnel burial depth is 45 m. The length is taken as 40 m. The upper surface of the model is a free edge. The surrounding boundary and the bottom are set as horizontal and vertical constraints. Respectively, a uniform load of 1.15 MPa is applied to the upper surface of the model. The finite element model established is shown in **Figure 1**, and the units used in the model are all international units.

The actual construction of this tunnel is basically constructed by the full section method, and only a very small part of the fault fracture zone is excavated by the CRD method (cross-central diaphragm wall method). Based on the model established, the excavation method for this simulation is excavated by the full section method. The initial support and second lining are simulated by solid units. In the actual construction process, the thickness of C25 shotcrete for initial support is 30 cm, and the thickness of C30 reinforced concrete structure for secondary lining is 50 cm.  $\phi 42 \times 4$  mm grouting conduit is used as the system anchor, with length 6 m, longitudinal spacing 0.5 m and circumferential spacing set to 1.0 m. It's elastic modulus is 205 GPa with radius  $r = 0.012$  m. The tunnel second lining and anchor are shown in **Figure 2**.

**Table 1.** Tunnel Class IV surrounding rock parameters.

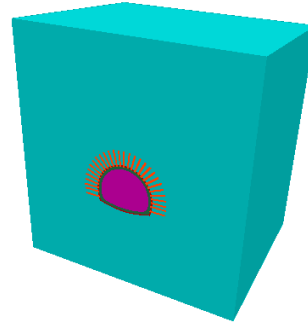
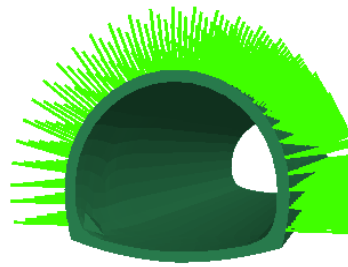
Rock	Modulus of elasticity E/GPa	Poisson's ratio	Severe/ (KN·m <sup>-3</sup> )	Cohesion c/MPa	Angle of internal friction $\phi/(\circ)$
Sandstone	12.6	0.24	20.2	4.45	46.52
Mudstone	9.25	0.18	21.0	1.51	38.48

**Table 2.** Lining mechanical parameters.

Type of support	Density (kg·m <sup>-3</sup> )	Modulus of elasticity/GPa	Uniaxial compressive strength/MPa	Poisson's ratio
C25 concrete	2570	22.5	11.5	0.21
C30 second lining	2500	30.5	21.3	0.20

**Table 3.** Mechanical parameters of anchor rods.

Modulus of elasticity/GPa	Poisson's ratio	Y-direction moment of inertia/m <sup>4</sup>	Z-direction moment of inertia/m <sup>4</sup>	Polar moment of inertia/m <sup>4</sup>
205	0.33	$3.05 \times 10^{-8}$	$3.05 \times 10^{-8}$	$5.95 \times 10^{-8}$

**Figure 1.** Tunnel model.**Figure 2.** Secondary lining and anchors.

### 3.2. Tunnel Control Points Layout

After the numerical simulation, the stress redistribution and displacement variation of the surrounding rock will be presented in the cloud map. The section at 50 m from the tunnel opening is taken as the control section, and the control points on the section are laid out as shown in **Figure 3**.

## 4. Numerical Simulation Calculation Results Analysis

In the proposed model, the tunnel width direction is x-direction, the length direction is y-direction, and the vertical direction is z-direction.

### 4.1. Analysis of the Numerical Simulation Results of the Initial Support

#### 4.1.1. Displacement in z-Direction

After the end of tunnel excavation, the vertical displacement cloud diagram of the section is shown in **Figure 4**. The initial stress of the surrounding rock is released, followed by the redistribution of stress, which leads to the deformation of the surrounding rock, showing an overall trend of sinking of the vault, bulging of the arch foot, inward extrusion and contraction of the side walls on both sides. As can be seen from the figure, after the initial support is carried out after

excavation, as the palm face continues to advance, the distance between the section and the palm face gradually increases, and the displacement of each characteristic point on the section shows a trend of first increasing and then gradually stabilizing. After the initial support is carried out and the displacement of each characteristic point reaches convergence, the settlement value of the top of the arch is 24.372 mm, the left and right side walls is 14.5 mm, the settlement value of the left and right shoulders is 17.5 mm, the foot of the arch and the bottom of the arch are uplifted respectively, but the uplifted value of the foot of the arch is larger, its uplifted value is 9.5 mm, and the bottom of the arch is 7.3015 mm.

#### 4.1.2. Vertical Stress

The vertical stress at this section is shown in **Figure 5**. When the distance between the support section and the palm face increases, the stress of the initial support also increases and eventually tends to converge. The stress value at the bottom of the arch is smaller when the full section method is constructed. In this section, the stress value at the bottom of the arch is 1.24 MPa, and the stress value at the top of the arch is 1.2 MPa. Due to the sinking of the top of the arch and the bulging of the bottom of the arch, the stress concentration at the left and right side walls and the foot of the arch is larger, and the stress value is slightly larger than other places. The stress value at the left and right side walls is 36.25 MPa, the stress value at the left and right shoulders is 22.5 MPa, and the stress value at the left and right foot of the arch is 42.5 MPa.

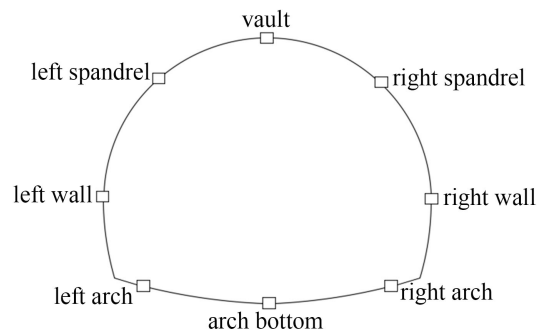


**Figure 3.** Tunnel support feature points.

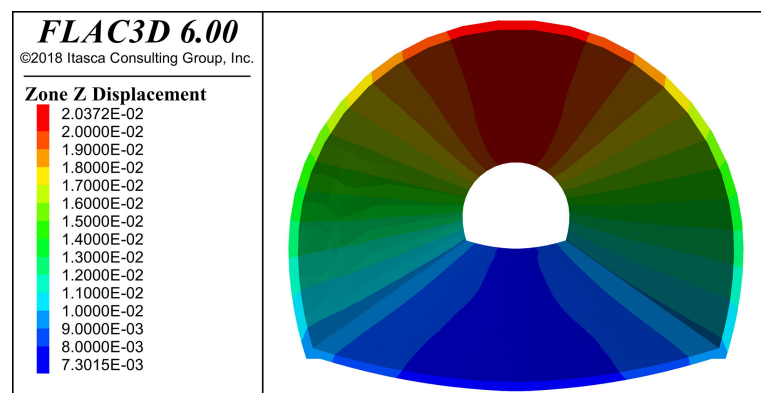


**Figure 4.** Initial support displacement in z-direction.

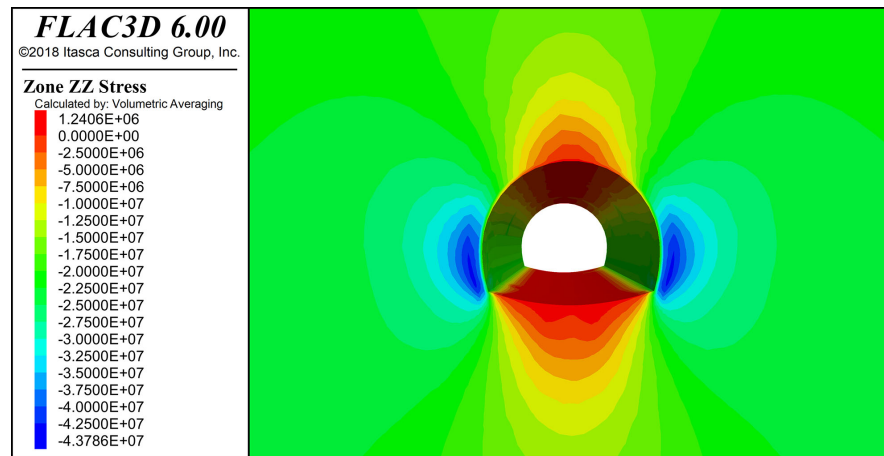


**Figure 5.** Initial support vertical stress.

## 4.2. Analysis of Secondary Lining Numerical Simulation Results

### 4.2.1. Displacement in z-Direction

The secondary lining of the tunnel will be carried out when the deformation of the surrounding rock and initial support is stable and the rate of deformation of the peripheral displacement decreases and has a tendency to slow down [14], and the secondary lining of the Zihong tunnel, on which this study is based, was used about 24 days after the end of the initial support. The displacement after the second lining is shown in **Figure 6**, with the maximum value of 8.319 mm for the top of the arch sinking, the minimum value of 5.137 mm for the bottom of the arch, 7.35 mm for the shoulder of the arch, and 5.25 mm for the left and right arches. Relative to the initial support, the displacement of each characteristic point after the second lining has been reduced significantly and basically shows a stable situation.

### 4.2.2. Vertical Stress

As shown in **Figure 7**. During the construction of the full-section method, after the secondary lining, the left and right side walls, and left and right arch footings still show a large stress concentration. The stresses at the left and right arch footings, left and right side walls are 16 MPa and 9.5 MPa respectively. According to the simulation results and field monitoring results, the location of the vertical stress when the basic convergence is 30 m from the palm face. Compared with the initial support, the pressure on the surrounding rock borne by the secondary lining is smaller, which fully follows the construction principle of the new Austrian method and plays the role of safety reserve.

## 4.3. Anchor Shaft Force Analysis

In the excavation using the full section method, the axial force of the anchor rods will also increase gradually as the excavation progresses. By analyzing the displacement and stress of the above characteristic points, the left and right side walls and the left and right arch foot will tend to contract inward, so the axial

force of the anchor rod will also show the maximum at these two characteristic points. From **Figure 8**, it can be seen that the axial force is the smallest at the top of the arch, and the values are larger at the left and right side walls and the foot of the arch, and the axial force of the anchor rod shows positive values in the whole section.

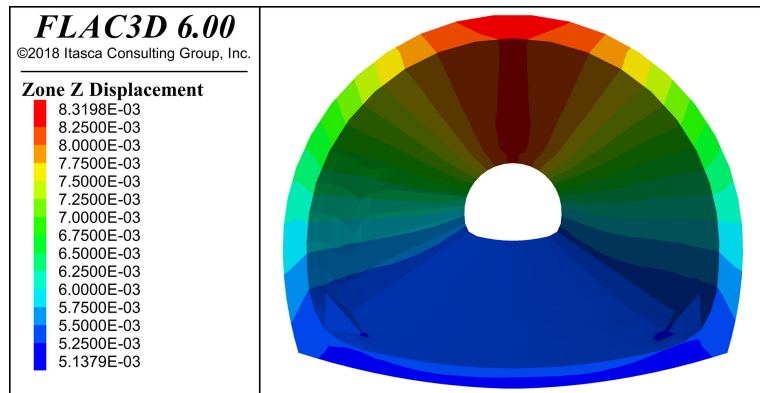


**Figure 6.** Secondary lining displacement in z-direction.

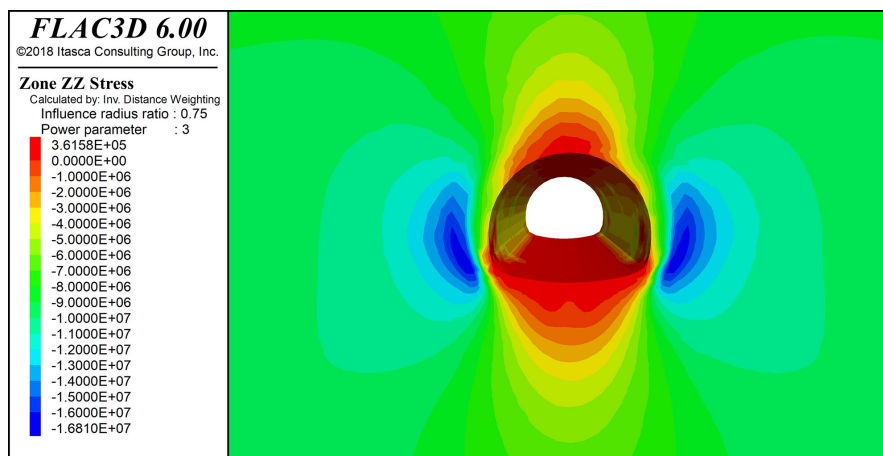


**Figure 7.** Secondary lining vertical stress.

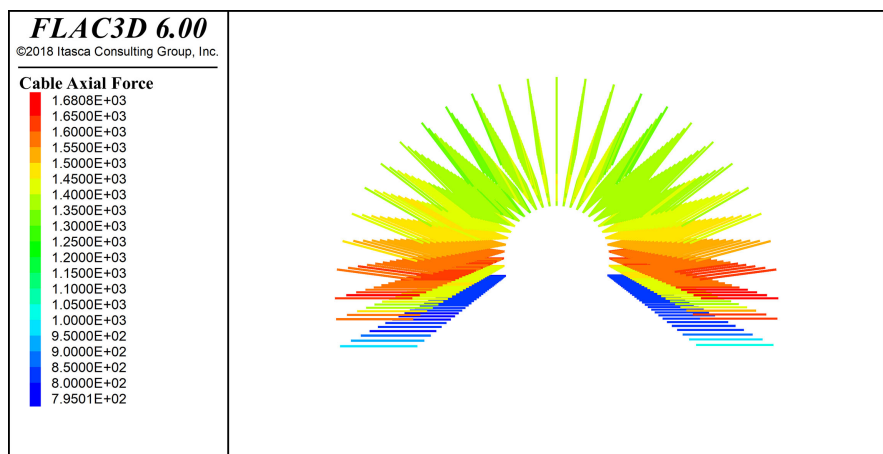


**Figure 8.** Anchor shaft force.

### 4.4. Plastic Zone Distribution

As shown in **Figure 9**. In the tunnel excavation with using the full section method, the plastic zone damage of the surrounding rock is symmetrically distributed left and right, with the axis being the tunnel centerline. There is almost no plastic damage in the vault area as well as near the arch base. In the final results of the simulation, the maximum value of the equivalent plastic deformation rate is 0.00275.

### 5. Support Embodied Field Monitoring and Analysis

The vertical displacement, vertical stress and horizontal stress of the initial support at the characteristic points of the tunnel monitoring section are shown in **Figures 10-12**, respectively. With the distance between the section and the palm face gradually increasing, the displacement and stress of the initial support body of monitoring have increased to a certain extent, when the section is about 30 meters away from the palm face, the displacement and stress gradually tend to converge,

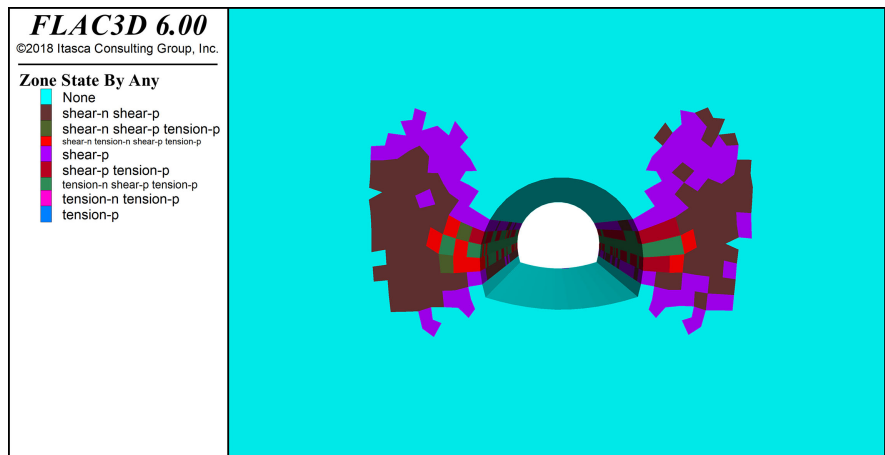


**Figure 9.** Plastic zone damage.

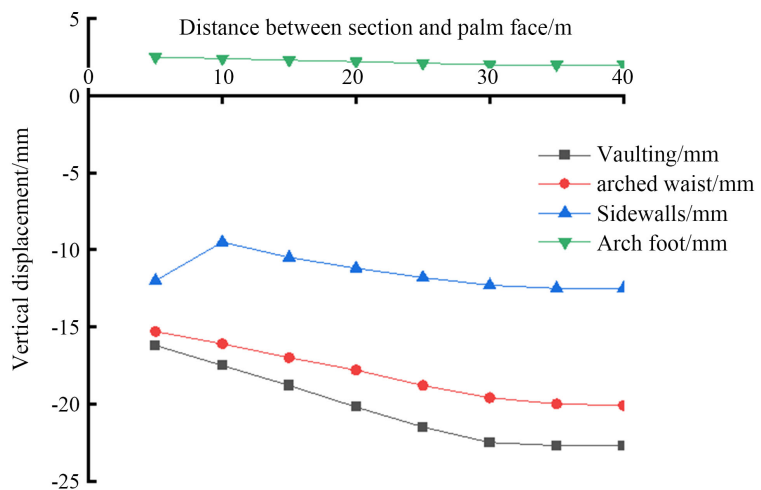


**Figure 10.** Vertical displacement curve of initial support of characteristic points.

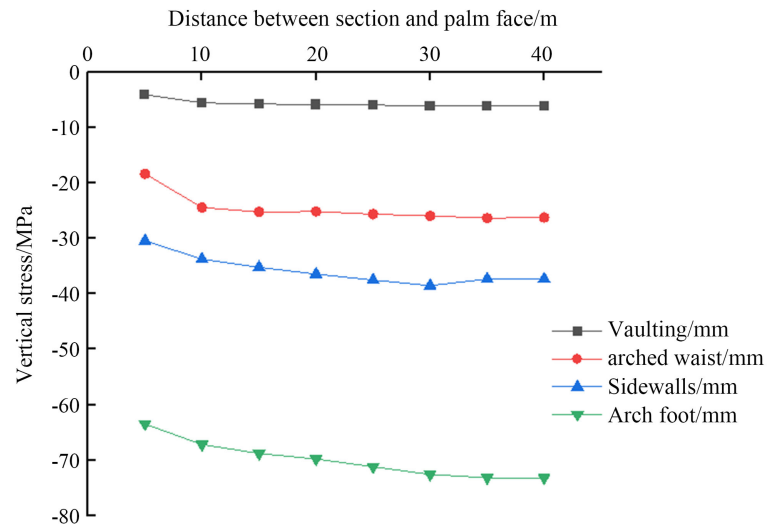


**Figure 11.** Vertical stress curve of initial support of characteristic points.

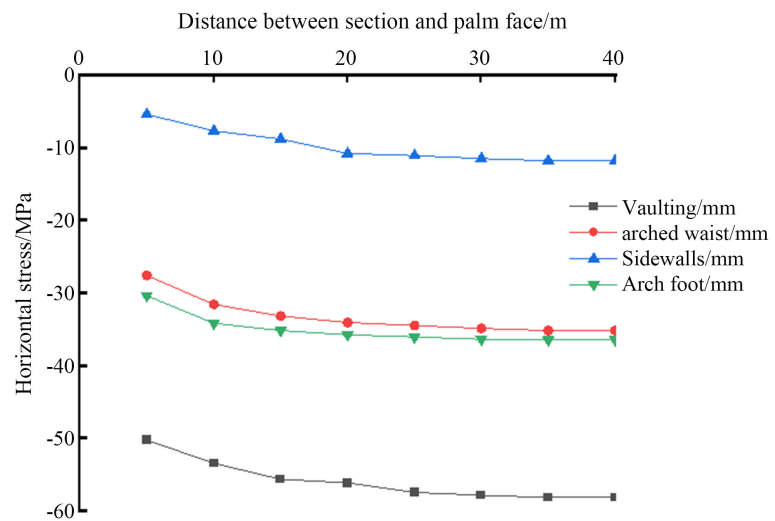


**Figure 12.** Horizontal stress curve of initial support at characteristic points.

the final convergence value of the displacement of the vault is 22.7 mm, which is consistent with the numerical. The final convergence value of the displacement of the vault is 22.7 mm, which is basically consistent with the numerical simulation results, but the simulation results of the vertical displacement and stress of the surrounding characteristic points of the tunnel section are slightly lower than the field monitoring results, which may be due to the fact that the groundwater and joints are not taken into account in the simulation calculation process. Overall, by comparing the simulation and field monitoring, we can conclude that the simulation results basically meet the requirements.

## 6. Conclusions

In this paper, the initial support and secondary lining of the tunnel were analyzed in terms of displacement, stress, plastic zone damage and axial force of

anchors by using Flac3D finite difference program and full section method excavation in combination with field engineering examples, and the following conclusions were obtained.

1) According to the stresses applied to the surrounding rock, the stresses applied at the sidewalls and the foot of the arch are higher, therefore, under high load pressure, the damage of the lining is most likely to start at the sidewalls and the foot of the arch, so extra attention should be paid to the support at these two characteristic points during the construction.

2) From the above numerical simulation, the absolute values of stresses and displacements are smaller from excavation and support to the final stable convergence, both for the stresses, vertical displacements and anchor axial forces of the initial support, and for the displacements and stresses of the secondary lining.

3) Using this method for excavation and support will give full play to the bearing capacity of the surrounding rock itself, with the surrounding rock and initial support playing the main bearing role, and in this grade of surrounding rock, the secondary lining will be used as a safety reserve, fully following the support concept of the new Austrian method.

4) In the numerical simulation, because the surrounding rock is often discontinuous medium, so it may be affected by the top slab water, geological structure and groundwater. The next step can be combined with geological structure, top slab water and groundwater on the surrounding rock for more in-depth research.

## Acknowledgements

This research was funded by National Natural Science Foundation of China (51974104).

## Conflicts of Interest

The authors declare no conflicts of interest regarding the publication of this paper.

## References

- [1] de F. Amorim, D.L.N., Proença, S.P.B. and Flórez-López, J. (2014) Simplified Modeling of Cracking in Concrete: Application in Tunnel Linings. *Engineering Structures*, **70**, 23-35. <https://doi.org/10.1016/j.engstruct.2014.03.031>
- [2] Jia, J.Q., Wang, H., Li, J., *et al.* (2010) Stability Analysis of Tunnel Support Structures under Complex Conditions. *Geotechnics*, **31**, 3599-3603+3618.
- [3] Di, C. (2021) Research on the Mechanism of Secondary Lining Cracking and Management Measures in Linpanshan Tunnel. Master's Thesis, Xi'an University of Architecture and Technology.
- [4] Huang, H.W., Liu, D.J., Xue, Y.D., *et al.* (2013) Numerical Analysis of Tunnel Liner Crack Cracking Based on Extended Finite Elements. *Journal of Geotechnical Engineering*, **35**, 266-275

- 
- [5] Zhang, Z., Zhao, C., et al. (2022) Research on the Stability of Shallow-Buried Large Cross-Section Tunnel by Construction Method Conversion. *Frontiers in Earth Science*, **10**, Article ID: 831169. <https://doi.org/10.3389/feart.2022.831169>
- [6] Zhang, X., Wei, C. and Zhang, H. (2021) Analysis of Surrounding Rock Creep Effect on the Long-Term Stability of Tunnel Secondary Lining. *Shock and Vibration*, 2021, Article ID: 4614265. <https://doi.org/10.1155/2021/4614265>
- [7] Fang, Q., Zhang, D.L., Wang, Y.Y., et al. (2011) Study of Contact Pressure between Primary Support and Second Lining in High-Speed Railroad Tunnels. *Journal of Rock Mechanics and Engineering*, **30**, 3377-3385.
- [8] Shao, Z.S., Zhang, Y.L., Wang, X.Y., et al. (2016) Analysis and Optimization of reasonable Support Timing for Second Lining of Large-Span Soft Rock Tunnel. *Journal of Underground Space and Engineering*, **12**, 996-1001.
- [9] Kang, H.B., Xiong, W.L., Zhao, G.Y., et al. (2021) Deformation Analysis of Tunnel Excavation Surrounding Rock through Coal Seams and Faults. *Science, Technology and Engineering*, **21**, 13148-13154.
- [10] Zhao, Q.C. (2018) Research on Stress Characteristics and Drainage Prevention Technology of Large Section Road Tunnel Lining Structure in High Pressure Water-Rich Area. Master's Thesis, Southwest Jiaotong University.
- [11] Wu, C., Huang, L., Chen, Z.T., et al. (2018) Model Tests on Force Characteristics of Secondary Lining in Large Section Highway Tunnels. *Tunnel Construction*, **38**, 977-985. (In English and Chinese)
- [12] Xu, D.Q. and Xue, Y.F. (2018) Optimization Analysis of the Elevation Arch of Class IV Surrounding Rock Section of Highway Ridge Tunnel Based on Field Monitoring and Numerical Simulation. *Science, Technology and Engineering*, **18**, 83-88.
- [13] Cheng, Y.Q. (2015) Analysis of Mechanical Properties of Construction Stage of Soft and Weak Surrounding Rocks. Master's Thesis, Lanzhou Jiaotong University.
- [14] Luo, Y.B. and Chen, J.X. (2021) Timing of Secondary Lining in Large-Span Highway Loess Tunnels under Viscoelastic Conditions. *Journal of Chang'an University (Natural Science Edition)*, **41**, 86-95.